Repositório ISCTE-IUL

Cost, power consumption and performance analysis in SDM ROADM architectures for uncoupled spatial channels

Marco Q. Silva[2], Luís G. Cancela[1,2], and João L. Rebola[1,2]

[1] Optical Communications and Photonics Group, Instituto de Telecomunicações, Lisbon, Portugal
[2] Department of Information Science and Technology, Instituto Universitário de Lisboa (ISCTE-IUL), Portugal
Email: mqsas@iscte-iul.pt; luis.cancela@iscte-iul.pt; joao.rebola@iscte-iul.pt

Abstract— **Currently optical networks are reaching their maximum transport capacity. Different solutions can be used to overcome this capacity limit, but we are going to study, in particular, space division multiplexing (SDM). To use SDM, the reconfigurable optical add/drop multiplexers (ROADMs) need to be adapted to support this multiplexing. In this paper we analyze four switching strategies used in SDM ROADMs and the respective SDM ROADM architectures. These strategies are explained and analyzed, for uncoupled scenarios, in terms of cost and power consumption. The impact of the physical layer impairments (PLIs) amplified spontaneous emission noise, non-linear interference, passband narrowing due to optical filtering and in-band crosstalk is also assessed, considering a cascade of SDM ROADMs with spatial and spatial-wavelength switching granularities. The PLI in-band crosstalk, has insignificant impact, in networks with a single spatial channel or in SDM networks with spatial granularity ROADM architecture, but in a SDM network with spatial wavelength granularity this PLI can lead to an OSNR penalty of around 2 dB, when the number of spatial channels is high. The other PLIs have similar impacts in all networks studied.**

Keywords— Amplified spontaneous emission noise, in-band crosstalk, non-linear interference, ROADMs, spatial division multiplexing.

I. INTRODUCTION

Optical transport networks are approaching their capacity limits, mainly due to new applications and services that require a huge amount of bandwidth, like video services. A solution to surpass this capacity crunch consists in using additional fiber bands other than the common C-band, the so-called multiband solution [1]. This is usually considered a short to medium term solution. A long-term solution is to use spatial-division multiplexing (SDM) in the optical domain, which leads to the concept of SDM-based optical networks [2,3]. Multicore fibers (MCF), multimode fibers (MMF) or multiple fibers (MF) in parallel are examples of SDM solutions for optical networks [2,3].

SDM-based optical networks use SDM reconfigurable optical add/drop multiplexers (ROADMs) to route optical signals along the network. SDM ROADM architectures with different switching strategies have been proposed in [2,3] for various SDM solutions (MCF, MMF and MF). In particular, architectures with spatial granularity, spatial and wavelength granularity, wavelength granularity and fractional spatial and wavelength granularity have been analyzed. In [2], besides, proposing SDM ROADMs architectures, a cost analysis between the various SDM ROADMs architectures solutions is also performed. More recently, in [4] the switching capacity

of several SDM ROADM architectures for the MF solution is assessed and compared.

In this work, the previous studies [2,3] are extended by providing a detailed cost and power consumption analysis of the various switching strategies for the MF solution, which is also known as the uncoupled scenario. In this analysis, the components of the express structure, as well as, of the add/drop (A/D) structure of the SDM ROADMs are detailed, and its cost alongside its power consumption are provided.

Moreover, in this work, a detailed performance analysis of a SDM ROADM based network, considering several physical layer impairments (PLIs), is presented. A Monte Carlo simulation analysis, as well as a simple analytical formalism based on the Gaussian approximation are used to assess the network performance.

This paper is organized as follows. Section II describes the SDM switching strategies and the SDM ROADM architectures used to implement these switching strategies. In section III, the cost and power consumption in SDM ROADM architectures are studied and compared with the reference ROADM architecture with a single spatial channel. In section IV, the PLIs impact in SDM ROADM architectures with spatial-wavelength and spatial granularities is assessed and discussed. In section V, the main conclusions of this work are presented.

II. SDM SWITCHING STRATEGIES AND ROADM ARCHITECTURES

The switching in ROADMs for SDM networks can be performed in two dimensions (space and wavelength). In this section, we are going to present and explain the four possible switching strategies in SDM ROADMs: space granularity, space-wavelength granularity, wavelength granularity and fractional space-full wavelength granularity [2,3]. Furthermore, for each one of the switching strategies, we are going to present and explain a possible SDM ROADM architecture implementation.
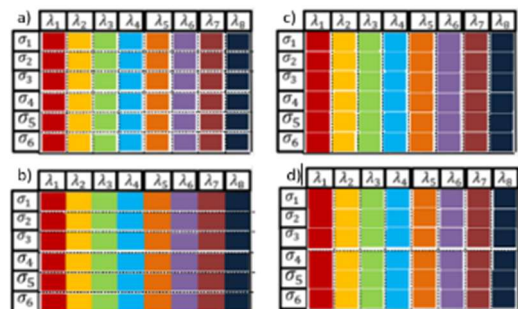

Fig. 1. SDM switching strategies (figure taken from [3]): a) space and wavelength granularity; b) space granularity; c) wavelength granularity; and d) fractional space and wavelength granularity. The dotted lines define the switching granularity of the different strategies.

In the space-wavelength granularity strategy represented in Fig. 1 a), the switching is performed between wavelength channels in any spatial channel. This strategy must use independent spatial and wavelength channels, hence, requiring uncoupled SDM fibers, such as the MF solution or the weakly-coupled MCF solution. This strategy is the one that leads to the most flexible switching architecture, since the switching is performed at the wavelength level granularity, but at the cost of more complexity [2,3].

For the ROADM architecture with spatial-wavelength granularity switching strategy, we propose a colorless, directionless and contentionless (CDC) Route & Select (R&S) architecture. In each direction of the ROADM, there is one input and one output WSS for each spatial channel. Each WSS is responsible for routing/receiving wavelength channels to/from any spatial channel of any direction and also M links towards the A/D structures. Each A/D structure corresponds to a WSS with multiple inputs and multiple outputs that has links to the input/output WSSs of all directions. There are M A/D structures in order to reduce the dimensions of the A/D WSSs that would be needed if only one A/D structure is used and also to avoid a single point of failure. The CDC R&S ROADM architecture found in current WDM networks is a specific case of the spatial-wavelength granularity with one spatial channel, i. e., $M = 1$ and it is our baseline scenario. In Fig. 2, a SDM ROADM architecture, with spatial-wavelength granularity, considering two directions $D = 2$ and two spatial channels, $M = 2$, is presented, and in Fig. 3, it is represented the A/D structure used in this architecture, formed by two 4×16 WSSs for the drop structure and two 16×4 WSSs for the add structure, considering 80 wavelengths per spatial channel, $N = 80$ and an A/D ratio of 20%.
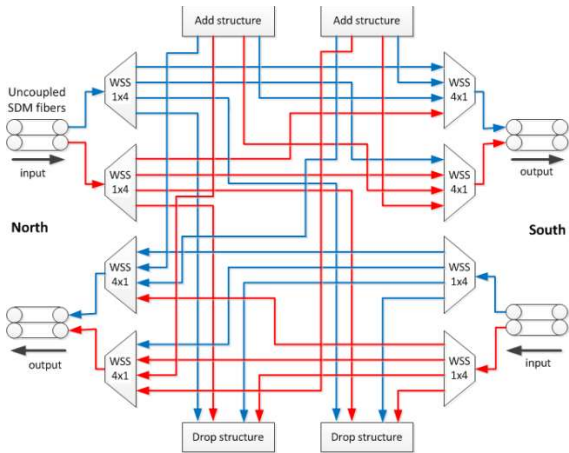

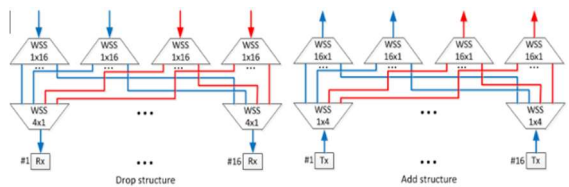Fig. 2. SDM ROADM architecture with spatial-wavelength granularity

Fig. 3. A/D structure for the SDM ROADM architecture with spatial-wavelength granularity

In the space granularity strategy, represented in Fig. 1 b), the switching is performed between spatial channels, by switching the entire WDM signal corresponding to a spatial channel [2,3]. The space granularity switching also demands uncoupled SDM fibers.

For the ROADM architecture with spatial granularity switching strategy, we have also proposed a CDC R&S

architecture. The express structure of this architecture has a single optical crossconnect (OXC) to perform the switching of the spatial channels between all directions, all spatial channels, and also to receive/send the spatial channels to the A/D structures [2,3]. The A/D structure has one WSS dedicated to each spatial channel in each direction. These WSSs are linked to multiple receivers and have also one link towards the add structure to return the wavelength channels that are not dropped. In Fig. 4, a SDM ROADM architecture, with spatial granularity is represented, considering two directions, $D = 2$, and four spatial channels, $M = 4$. The respective A/D structure is formed by four 1×17 WSSs for the drop structure and four 17×1 WSSs for the add structure, considering 80 wavelengths per spatial channel, $N = 80$ and an A/D ratio of 20%.
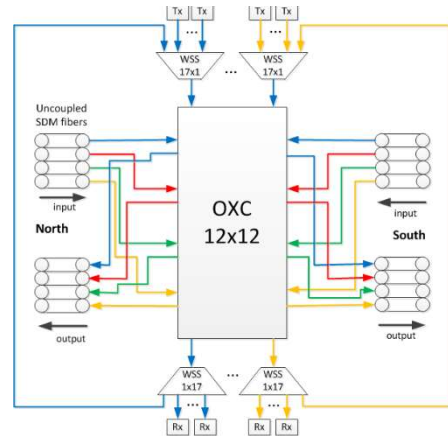

Fig. 4. SDM ROADM architecture with spatial granularity

In the wavelength granularity strategy, represented in Fig. 1 c), the switching is performed between groups of channels with the same wavelength, which form a spatial superchannel, i.e., all wavelength channels λ_n (with $n=1,..., 8$), forming a spatial superchannel in one direction, are switched together to another direction. A joint switch WSS must be used to perform this operation [2,3].

For the ROADM architecture with wavelength granularity switching strategy, we propose a CDC R&S architecture. In each direction of the ROADM, there is one input and one output joint switch WSS. Each joint switch WSS is responsible for routing/receiving a spatial superchannel to/from the joint switch WSSs of the other directions. Each joint switch WSS has also a link towards the A/D structure. There is one A/D structure for each direction responsible to A/D a spatial superchannel, which must also use joint switch WSS [2,3].

In the fractional space-full wavelength strategy, represented in Fig. 1 d), the switching is done between subgroups of channels with the same wavelength. For example, subgroup 1 composed by the wavelength channels in the spatial channels $\sigma_1, \sigma_2, \sigma_3$ and subgroup 2 composed by $\sigma_4, \sigma_5, \sigma_6$. This strategy is very similar to the wavelength strategy represented in Fig. 1 c), still supported by spatial superchannels, but with this strategy, the degree of spatial granularity is increased.

For the ROADM architecture with fractional space-full wavelength granularity switching strategy, we propose also a CDC R&S architecture. In each direction of the ROADM, there are G (corresponding to the number of superchannels groups) input and output joint switch WSSs. Each input joint switch WSS is responsible for routing the spatial superchannel from its group to the output joint switch WSSs or to the drop structure. The output joint switch WSSs are responsible for

receiving the superchannels from the input WSSs and from the add structure. There is one A/D structure for each direction. This A/D structure has one joint switch WSS per group. Each joint switch WSS is responsible for A/D the spatial superchannels from their corresponding groups.

III. Cost per bit and power consumption analysis

In this section, we are going to analyze the SDM ROADM architectures proposed in the previous section in terms of cost per bit and power consumption.

To perform this analysis, first we need to count the number of components used in the express structure and in the A/D structure. In Tables 1 and 2, the expressions used to determine the number of components in each structure are presented.

From Tables 1 and 2, it is possible to observe that the architecture with spatial granularity is the architecture that uses less hardware in the express structure, and in the A/D structure. However, it is the less flexible architecture. The OXC in the architecture with spatial granularity can be implemented with micro-electro-mechanical systems (MEMS) or WSSs [1,2]. In this work we assume that the OXC is implemented with MEMS, and for simplicity, we also assume that MEMS have the same cost as WSSs.

The architecture with spatial-wavelength granularity is the architecture that needs more hardware in both, express and A/D structures due to its higher switching flexibility. The architectures with wavelength and fractional space-full wavelength granularities use less hardware and are also less flexible than the architecture with space-wavelength granularity, but in these two architectures, the number of transponders is much higher.

The cost for the WSSs and joint switches WSSs presented in Table 3 were obtained following the method explained in [2] and normalized to the cost of the 1×10 twin WSS. The transponder cost is not considered in [2], and therefore, the transponder cost has been taken from [5], where it was shown that this component has a cost 4.5 times higher than a 1×4 WSS. Using this information, a 1×10 twin WSS has a normalized cost 2.3 times more expensive than a twin 1×4 WSS.

In Fig. 5, the relative cost per bit as a function of the number of ROADM directions (D) and number of spatial channels (M), for all the SDM ROADM architectures studied and for the baseline scenario is shown. The relative cost per bit of these architectures is obtained by normalizing the total ROADM cost to the cost of the baseline scenario (i.e. $M = 1$) considering four directions, $D = 4$. So, for example, if the capacity is increased by a factor of 7 ($M = 7$), the ROADM cost is divided by a factor of 7 to achieve the relative cost per bit. From Fig. 5, considering the same number of directions, it can be concluded that an increase of the number of spatial channels, M, causes: 1) an increase of the cost per bit of the architectures with spatial and spatial-wavelength granularity, 2) a decrease of the cost per bit of the architecture with fractional space-full wavelength granularity and 3) practically does not affect the cost per bit of the wavelength granularity architecture.

Table 1: Number of components and their size in the express structure for each of the SDM architectures.

Granularity	Number of components	inputs	outputs
Spatial	$N_{OXC} = 1$	$M \cdot (D + 1)$	$M \cdot (D + 1)$
Spatial-Wavelength	$N_{WSS} = 2MD$	1	$D \cdot M$
Wavelength	$N_{jointWSS} = 2D$	M	$D \cdot M$
Fractional space-full wavelength	$N_{jointWSS} = 2DG$	$\frac{M}{G}$	$\frac{M}{G} \cdot [(D - 1) \cdot G + 1]$

Table 2: Number of components and their size in the A/D structure for each of the SDM architectures.

Granularity		Spatial	Spatial-wavelength	Wavelength	Fractional space-full wavelength
# A/D structures per architecture ($N_{A/D}$)		2	$2 \cdot M$	$2 \cdot D$	$2 \cdot D$
# WSSs per A/D structure	# Input WSS drop/ # output WSS add	M	$D \cdot M$	1	G
	# Output WSS drop/ # input WSS add		$A/D_{ratio} \cdot N$		
# inputs	# Input WSS	1	1	M	$\frac{M}{G}$
	# Output WSS		$D \cdot M$		
# outputs	# Input WSS	$A/D_{ratio} \cdot N$	$A/D_{ratio} \cdot N$	$M \cdot A/D_{ratio} \cdot N$	$A/D_{ratio} \cdot N \cdot \frac{M}{G}$
	# Output WSS	$A/D_{ratio} \cdot N + 1$	1		
# transponders		$N_{A/D} \cdot A/D_{ratio} \cdot N$	$M \cdot A/D_{ratio} \cdot N \cdot N_{A/D}$	$A/D_{ratio} \cdot N \cdot \frac{M}{G} \cdot N_{A/D} \cdot G$	

Table 3: Hardware cost.

Twin WSS	Cost	Power (W)
1×2	0.25	50
1×4	0.5	100
1×10	1	150
1×20	1.5	200
1×40	2.25	240
Joint switch WSS		
20 ports	1	100
40 ports	1.5	120
80 ports	2.25	140
160 ports	3.375	160
320 ports	5.0625	180
100 Gbit/s transponder	1.14	120

When the number of directions is increased, a substantial increase in the cost per bit of all architectures is observed, except for the architecture with spatial granularity, where the cost increase is not so pronounced. From Fig. 5, it can be also concluded that the architectures with wavelength and fractional space-full wavelength granularity can lead to some cost advantages, in uncoupled scenarios, when $D < 8$ and $M = 19$, because, in these conditions, they are less expensive than the architecture with space-wavelength granularity.
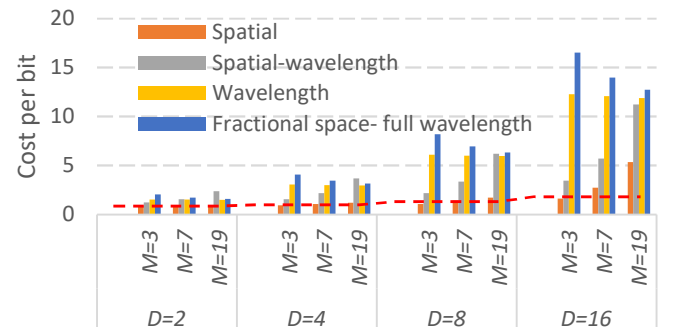

Fig. 5. Cost per bit of the SDM ROADM-based architectures normalized to the cost per bit of the baseline scenario with 4 directions, as a function of the number of ROADM directions, D, and number of spatial channels, M.

In Fig. 6, the power consumption, in kilowatt (KW), as a function of D and M, for all SDM ROADM architectures studied, normalized to the cost of the baseline scenario with 4 directions is shown. The power consumption for the baseline scenario is not shown in Fig. 6, because it is too low. The power consumption for the baseline scenario varies from 9.9 kW ($D = 2$), to 21.1 kW ($D = 16$). For all architectures it is observed that, a higher number of directions or number of spatial channels causes a higher power consumption.

The increase of the number of spatial channels leads to a more significant power consumption for the architecture with spatial-wavelength granularity. For example, with $D = 8$, the increase of the number of spatial channels from 7 to 19 leads to a power consumption, 2.9, 4.8, 2.7 and 2.5 times higher, respectively, for the architectures with space, spatial-wavelength, wavelength and fractional space-full wavelength granularities. The increase of the number of directions causes a higher power consumption increase for the architectures with wavelength and fractional space-full wavelength granularities.
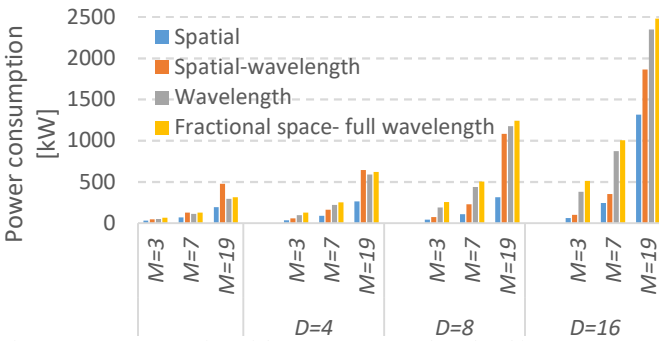

Fig. 6. Power consumption of the SDM ROADM-based architectures as a function of the number of ROADM directions, D, and number of spatial channels, M.

From Fig. 6, it can be concluded that the architectures with wavelength and fractional space-full wavelength granularity can lead to advantages regarding the power consumption when $D < 8$ and $M = 19$, in comparison with the architecture with space-wavelength granularity.

IV. PLIs ANALYSIS IN ARCHITECTURES WITH SPATIAL AND SPATIAL-WAVELENGTH GRANULARITY

In this section, we perform an analysis of the impact of the most relevant PLIs in the performance of a cascade of SDM ROADMs. In particular, we consider the ASE noise, the NLI, the passband narrowing effects and the in-band crosstalk. This analysis is performed both analytically for the architecture with spatial and spatial-wavelength granularity, and with a Monte Carlo simulation only for the spatial-wavelength architecture. The architectures with wavelength and fractional space-full wavelength granularities have not been studied, because in the previous section, we have concluded that these architectures do not bring significant cost and power consumption advantages in the majority of the uncoupled scenarios studied.

A. ROADM cascade without in-band crosstalk

In this sub-section, the ASE noise, NLI effect, and passband narrowing are assessed analytically for the architectures with spatial and spatial-wavelength granularity and by Matlab simulation for the architecture with spatial-wavelength granularity.

The PLIs analytical and simulated analysis is done by assessing the optical signal-to-noise ratio (OSNR) obtained for a network with the following parameters: optimum signal power p_s, bit rate R_b =100 Gbit/s, line bit rate $R_{b,l} = 120$ Gbit/s, quaternary phase-shift-keying (QPSK) modulation, optical bandwidth B_o =30 GHz, amplifier figure noise $F_n = $ 6.9 dB, frequency of the central channel ν_o =193.8 THz, fiber section length L_{sec} = 80 km, attenuation coefficient α=0.2 dB/km, pre-amplifier gain $G_{pre_{amp}}$ = 16 dB, post amplifier gain $G_{post_{amp}}$ =19.2 dB for the architecture with spatial granularity or 20.4 dB for the architecture with spatial-wavelength granularity, symbol rate R_s = 30 GBaud, 80 wavelength channels per spatial channel, fiber dispersion coefficient D_s = 18 ps/nm/km, nonlinear fiber coefficient γ = 1.1 $W^{-1}km^{-1}$, channel spacing of 50 GHz, Super-Gaussian passband and stopband filters of 4th order with -3 dB bandwidth of 45 GHz and different isolations [6].

For the analytical assessment, the ASE noise power is calculated using [7], the passband narrowing effect is obtained following [8] and the NLI effect is calculated with the expressions presented in [9].

In Fig. 7, the model used to study and simulate a cascade of CDC R&S SDM ROADMs with spatial-wavelength granularity is presented. In Fig. 7, $s_{add}(t)$ is the QPSK signal generated by the optical transmitter and $s_{exp,j}(t)$ are the signals at the output of each jth ROADM (with j=1, ..., n_r) along the network, where n_r is the total number of ROADMs in the cascade. In the simulation model depicted in Fig. 7, the first ROADM is used to add the signal into the network. At the output of this ROADM, the signal already went through 3 WSSs and one optical amplifier that adds ASE noise to the signal. The next ROADMs are used as express ROADMs,
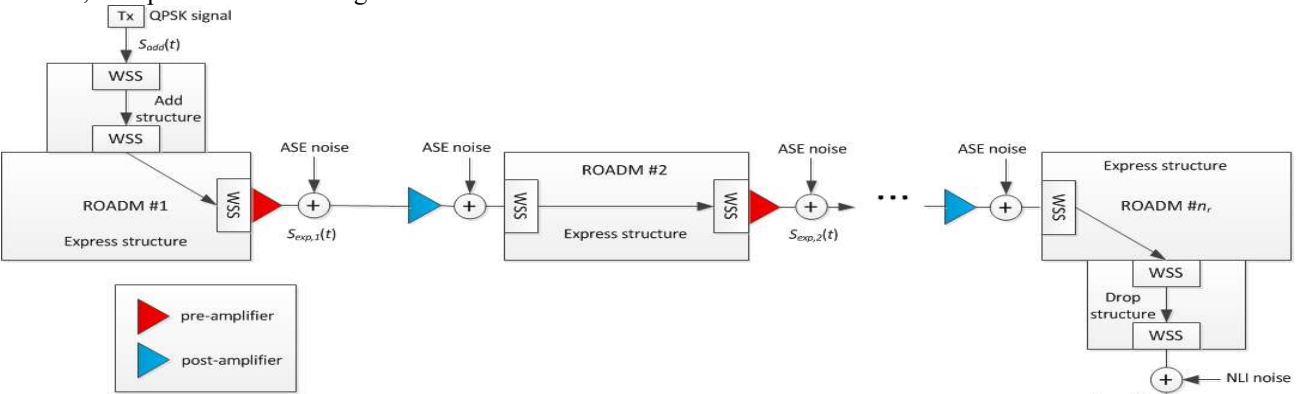

Fig. 7. Simulation model of a cascade of n_r ROADMs with spatial-wavelength granularity architecture, considering the ASE noise, filtering effects and NLI.

i.e., the signal is expressed from a ROADM input to a ROADM output, and in this case, the signal goes through 2 WSSs and 2 optical amplifiers. Finally, the signal is dropped from the optical network in the last ROADM, where it goes through 3 WSSs and one amplifier. The optical amplifiers considered in the simulation and represented in Fig. 7 are assumed to perfectly compensate the network losses and add ASE noise to the signal. In the simulation, the ASE noise power is defined by setting the power of each sample function of noise with the expressions provided in [7]. Furthermore, the NLI noise of the fiber is computed using the expressions shown in [9] and added at the input of the coherent optical receiver, as indicated in Fig. 7.

In this simulation, the passband narrowing was studied and compared with the results of [8], concluding that the OSNR penalty caused by this PLI is insignificant (in a cascade of 10 ROADMs, the OSNR penalty due to passband narrowing is 0.2 dB). The OSNR penalty is the difference between the OSNR calculated considering the passband narrowing effect and the OSNR calculated with only the ASE noise, for a specific target BER.

In Fig. 8, it is shown, the OSNR at the signal bandwidth, obtained by simulation, as a function of the number of ROADMs, with and without NLI. As can be observed in Fig. 8, the OSNR decreases as the number of cascaded ROADMs grows due to an increase of ASE noise power, NLI and filtering penalties. From Fig. 8, we can also confirm that for 10 cascaded ROADMs, an OSNR of 14.4 dB is obtained, which is in agreement with the values obtained analytically. The difference of OSNR between a system with and without NLI when the optimum signal power is considered is 1.76 dB as it should be [9].

In order to keep the system performance, we have considered that the system margin needs to be higher than 3 dB, which corresponds to a minimum OSNR of 10.2 dB. Therefore, a signal can cross 23 cascaded ROADMs without reaching the minimum OSNR, when considering the effects of ASE noise, passband narrowing and NLI.

B. ROADM cascade with in-band crosstalk

The crosstalk is a PLI, that is caused mainly by the imperfect isolation of optical components that causes power leakages leading to signal degradation at the receiver [11]. These power leakages are the interfering terms that will impair the selected signal. In this work, we only consider the in-band crosstalk, that occurs when the interfering signals have the same nominal wavelength of the selected signal [10]. The first step to study the in-band crosstalk is to obtain the number of interfering terms in the SDM architectures.
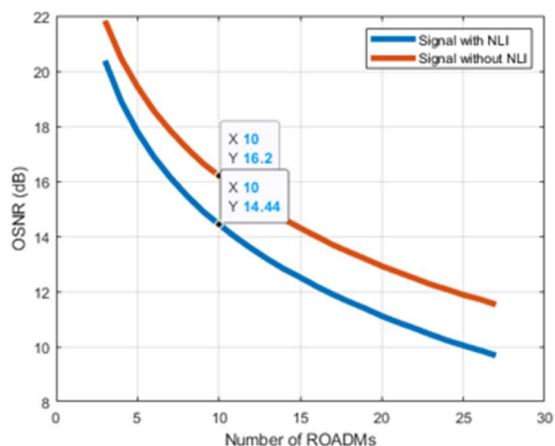
Fig 8. OSNR measured at the signal bandwidth as a function of the number of ROADMs, without and with NLI.

In Table 4, the expressions that allow calculating the number of 1st and 2nd order in-band interfering terms at the ROADM output or at the receivers input for the worst-case scenario (scenario where all wavelength channels are extracted and added) in the baseline, spatial-wavelength and spatial granularities architectures, are presented. The order of the interfering terms represents the number of times that a interfering term beats the WSS isolation. The architecture with less in-band interfering terms is the architecture with spatial granularity. This architecture has always one in-band interfering term, because the switching in this architecture is performed by the OXC, which has very high isolation, since it was assumed a MEMS implementation. The architecture with more in-band interfering terms is the architecture with spatial-wavelength granularity and the number of interfering terms in this architecture increases with the number of spatial channels. The baseline architecture is a special case of the spatial-wavelength granularity architecture, by considering $M = 1$. The derived expressions of the baseline scenario have been validated and are in agreement with the expressions presented in Table 4.1 of [10].

To assess the OSNR penalty due to in-band crosstalk analytically, we consider that the in-band crosstalk can be modeled as an additive noise with a Gaussian distribution as in [11] with the OSNR given by:

$$osnr_{XT} = \frac{p_s}{p_{ase} + p_{NLI} + p_{XT}} \qquad (1)$$

where p_s is the signal power, p_{ase} the amplified emission spontaneous noise power, p_{NLI} non-linear interference power, p_{XT} is the interfering terms power. The OSNR penalty due to in-band crosstalk obtained analytically, for 10 cascaded ROADMs, in the architecture with spatial-wavelength granularity with a WSS isolation $A = -30$ and $A = -25$ dB is, respectively, 0.7 and 4.2 dB. For the architecture with spatial granularity with $A = -30$ and $A = -25$ dB, the OSNR penalty obtained is, respectively, only 0.1 and 0.4 dB. Considering the OSNR penalties due to in-band crosstalk, for a WSSs with isolation of -30 and -25 dB, the OSNR obtained analytically, at the optical receiver input after 10 cascaded ROADMs with $D = 16$, $M = 19$ and spatial-wavelength granularity architecture, is 13.8 and 10.2 dB. For the same scenario but using the architecture with spatial granularity, the OSNR is 14.9 and 14.7 dB. So, by considering the in-band crosstalk penalty, our analytical results show that the architecture with spatial granularity leads to an OSNR improvement of about 4.5 dB in relation to the spatial-wavelength architecture.

Table 4: Number of in-band interfering terms at the ROADM output and at the input of the optical receivers of the drop structure in the baseline, spatial-wavelength granularity and spatial granularity architectures.

Architectures	Baseline architecture/ Spatial wavelength granularity architecture	Spatial granularity architecture
# 2nd order interfering terms at the receivers input of the drop structure	$(D \times M) - 1$	-
# 2nd order interfering terms at the ROADM output	$((D - 1) \times M) + ((D \times M) - 1)$	-
# 1st order interfering terms at the ROADM output	-	1

The OSNR penalties predicted by simulation can be different from the ones predicted analytically, because the waveform distortion is not considered in the analytical analysis. Therefore, for the architecture with spatial-wavelength granularity, the impact of in-band crosstalk, is

studied more rigorously by simulation. The simulator model with in-band crosstalk is similar to the one presented in Fig. 7, but with the interfering terms summed to the signal. The number of interfering terms is obtained with the expressions of Table 4 and each interfering term is added to the main signal at the ROADM output or at the receiver input. Each in-band crosstalk signal is generated with the same characteristics of the primary signal (which is a QPSK signal), but for each interfering term, the bits are randomly generated. Each interfering signal is generated also with a phase difference and a time misalignment, in relation to the original signal. The time misalignment and phase difference are modelled as a uniformly distributed random variables, respectively, between $[0, T_s]$ and between $[0, 2\pi]$ as in [6]. A first order interfering term must go through one blocking filter that simulates a 1st order leakage in WSSs, whereas second order interfering terms must go through two blocking filters. The blocking filters are modelled using the Super-Gaussian stopband filter. In Fig. 9, the OSNR, Fig. 9 a), and crosstalk level, Fig. 9 b), as a function of the number of ROADMs, for $A = -25$ dB, 16 directions and different numbers of spatial channels are represented. In Fig. 9 a), it is possible to observe that the impact of in-band crosstalk on the OSNR is enhanced as the number of spatial channels grows. For $M = 1$ and 4, the in-band crosstalk impact is negligible. For $M = 8$, 16 and 19, after 27 cascaded ROADMs, the OSNR penalty due to in-band crosstalk is, respectively, 1.2 dB, 1.9 dB and 2 dB. For these cases, in Fig. 9 b), the crosstalk levels achieved at the end of the cascade of 27 ROADMs are -15.1 dB, -12.7 dB and -12.4 dB, respectively, for $M = 8$, 16 and 19. In [10], for the same crosstalk levels, the OSNR penalty obtained was, respectively, 1.2 dB, 1.8 dB and 2 dB, for QPSK signals, which is in a very good agreement with our results.
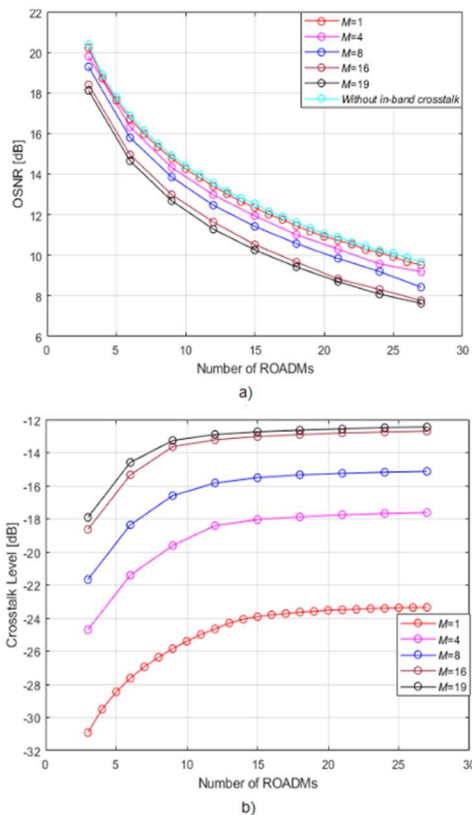

Figure 9. OSNR (a) and crosstalk level (b) as a function of the number of ROADMs for a system with ASE noise, passband narrowing due to

filtering, NLI and in-band crosstalk, for A= -25 dB, D=16 and a different number of spatial channels.

By comparing the OSNR shown in Fig. 9 a), for $D = 16$ and $M = 19$, for 10 cascaded ROADMs, with simulation results obtained for the spatial granularity architecture, the OSNR difference in presence of in-band crosstalk is 2.7 dB, which is much lower than the 4.5 dB calculated analytically. For a minimum OSNR of 10.2 dB and $A = -25$ dB (Fig. 9 a)), $D = 16$ and $M = 1, 4, 8, 16$ and 19, the signal can cross, respectively, 24, 21, 19, 16 and 15 ROADMs.

V. Conclusion

In this work, a detailed cost and power consumption analysis of a SDM ROADM based network for the uncoupled scenario (MF solution) is performed. We have concluded that the architectures with wavelength and fractional space-full wavelength granularities do not bring significant advantages in uncoupled scenarios, because they have a higher cost and power consumption than the architecture with spatial-wavelength granularity and are less flexible.

An assessment of the PLIs on a SDM network with ROADM architectures with spatial and spatial-wavelength granularity has been also performed. With this assessment, it was concluded that for a WSS isolation of -25 dB, the architecture with spatial granularity has a 2.7 dB higher OSNR than the architecture with spatial-wavelength granularity, after 10 cascaded ROADMs, but it is less flexible. We have also observed that in SDM ROADMs with spatial-wavelength granularity, the in-band crosstalk is much higher than in single spatial channels ROADMs, and that the OSNR penalty due to in-band crosstalk can reach 2 dB, for $M = 19$ and $D = 16$ cascaded ROADMs. In this case, the signal is able to cross 9 less ROADMs in comparison with the single spatial channel scenario.

ACKNOWLEDGMENTS

REFERENCES

[1] A. Napoli *et al.*, "Towards multiband optical systems," *Advanced Photonics Conference*, Paper NeTu3E.1, California USA, 2018.
[2] D. Marom *et al.*, "Survey of photonic switching architectures and technologies in support of spatially and spectrally flexible optical networking," *Journal of Optical Communications and Networking*, vol. 9, no. 1, pp. 1–26, Jan. 2017.
[3] D. Marom and M. Blau, "Switching solutions for WDM-SDM optical networks," *IEEE Communications Magazine*, vol. 53, no. 2, pp. 60–68, Feb. 2015.
[4] A. Anchal and D. Marom, "Practical SDM-ROADM Designs for Uncoupled Spatial Channels and their Switching Capacity", *in Proc. Opt. Fiber Commun. Conf. Expo.*, paper M1A.4, San Diego, CA, USA, 2019.
[5] J. Hernandez *et al.*, "Comprehensive model for technoeconomic studies of next-generation central offices for metro networks," *Journal of Optical Communications Networking*, vol. 12, no. 12, pp. 414–427, Dec. 2020.
[6] D. Sequeira, L. Cancela, and J. Rebola, "CDC ROADM design tradeoffs due to physical layer impairments in optical networks," *Optical Fiber Technology*, vol. 62, no. 102461, pp. 1-11, Jan. 2021.
[7] R. -J. Essiambre, G. Kramer, P. J. Winzer, G. J. Foschini and B. Goebel, "Capacity limits of optical fiber networks," *Journal of Lightwave Technology*, vol. 28, no. 4, pp. 662-701, Feb. 2010.
[8] A. Morea, J. Renaudier, T. Zami, A. Ghazisaeidi and O. Bertran-Pardo, "Throughput comparison between transparent networks," *Journal of Optical Communications and Networking*, vol. 7, no. 2, pp. A293–A300, Feb. 2015.
[9] P. Poggiolini and Y. Jiang, "Recent advances in the modeling of the impact of nonlinear fiber propagation effects on uncompensated coherent transmission systems," *Journal of Lightwave Technology*, vol. 35, no. 3, pp. 458-480, Feb. 2017.
[10] D. Sequeira, L. Cancela and J. Rebola, "Impact of physical layer impairments on multi-degree CDC ROADM-based optical networks," International Conference on Optical Network Design and Modeling (ONDM), pp. 94-99, Dublin, Ireland, May 2018.
[11] K. Ho, "Effects of homodyne crosstalk on dual-polarization QPSK signals," *Journal of Lightwave Technology*, vol. 29, no. 1, pp. 124-131, Jan. 2011.